films were not studied.

[7]O. T. Anderson, D. H. Liebenberg, and J. R. Dillinger, Phys. Rev. 117, 39 (1960).

[8]W. E. Keller, Phys. Rev. Lett. 24, 569 (1970). Also W. Keller reported [Proceedings of the Twelfth International Conference on Low Temperature Physics, Kyoto, Japan, 4-10 September 1970 (to be published), Abstract 6Z, p. 33] that preliminary measurements of the film thickness for a section of gravitationally driven film in which dissipation is occurring indicates no change in film thickness attributable to dissipation processes *per se*.

[9]The experimental technique has been extended to higher power and consequently larger temperature differences. The data for $\Delta T \geq 5$ mK deviate from the rest of the data presented here. Several effects must be considered at the higher power levels, including the stability of bath control to larger power inputs, a modification of the film-flow process related to evaporation along the film below the heater, and participation of the normal fluid component in the dissipation process. Further experiments are in progress.

[10]W. C. Knudsen and J. R. Dillinger, Phys. Rev. 91, 489 (1953). See also W. E. Keller, *Helium-3 and Helium-4* (Plenum, New York, 1969), p. 290.

[11]R. W. Cohen and B. Abeles, Phys. Rev. 168, 444 (1968).

[12]R. C. Clark, Phys. Fluids 12, 396 (1969).

[13]E. R. Huggins, Phys. Rev. Lett. 24, 573 (1970).

[14]E. R. Huggins, Phys. Rev. Lett. 24, 699 (1970).

# Propagation of Electron Cyclotron Waves Along a Magnetic Beach

G. Lisitano
*Institut für Plasma Physik, Garching, Germany*

and

M. Fontanesi and S. Bernabei
*Instituto di Scienze Fisiche, Laboratorio di Fisica del Plasma del Consiglio Nazionale delle Richerche, Milano, Italia*

(Received 1 February 1971)

The wave dispersion characteristic of whistler waves in a plasma is directly recorded as a function of the ratio of electron cyclotron frequency to wave frequency along their propagation path in a magnetic mirror. In the limit of small wavelengths the dispersion characteristic approaches that of plane waves in an unbounded plasma.

The dispersion relation of right-hand circularly polarized waves in plasma (whistler waves),

$$n^2 = \frac{k^2c^2}{\omega^2} = 1 + \frac{(\omega_p/\omega)^2}{\omega_b/\omega - 1}, \quad (1)$$

suggests an experimental study of these waves along a weakening magnetic field (magnetic beach). Here, $c$ is the speed of light, $k$ is the wave number, $\omega$ is the signal frequency, $\omega_p$ is the electron plasma frequency, and $\omega_b$ is the electron cyclotron frequency. Near electron cyclotron resonance, in the region $\omega_b/\omega \geq 1$, this dispersion relation, which is valid for an unbounded plasma, should also hold for free-space wavelengths several times larger than the transverse dimension of a laboratory plasma. In Eq. (1) the momentum-transfer collision frequency has been neglected and the angle between the direction of propagation and the static magnetic field is assumed to be zero.

The importance of experimental verification of Eq. (1) along a magnetic beach lies in the possibility of performing tests of validity for the microscopic progagation theory of the whistler mode with allowance for Landau damping, cyclotron damping, and plasma acceleration.[1-3] Until now it has been very difficult to study whistler-mode propagation in a laboratory plasma either because of large coupling losses of wave-exciting probes[2] or because of the complexity of separate excitation of circularly polarized waves.[4,5] Hitherto, measurements of $n(\omega_b/\omega)$ in a uniform magnetic field have had the disadvantages that in changing $\omega_b$ one is confronted with variations of the plasma parameters; or if $\omega$ is changed, the amplitude of the test wave varies depending on the coupling losses of the launching device used.[2,4,5]

In this Letter the validity of Eq. (1) in the limit of small wavelengths is confirmed by experimental data taken along a propagation path in a magnetic beach, in the vicinity of the resonance region $\omega_b/\omega \geq 1$. The wave-dispersion characteristic is directly recorded as a function of $\omega_b/\omega$ by sampling the whistler wave along its propagation path in the magnetic-mirror plasma. This

is possible since, by using a new wave coupling device, a relatively high level of whistler mode is coupled in the plasma.

The experiment was performed in a plasma generated in a magnetic mirror (mirror ratio 4:1) by a slow-wave rf plasma source,[6] consisting of a helical, slotted, metal tube fed with 150 W of cw power at 2.4 GHz. The argon plasma column, 3 cm in diameter and 1 m in length, is almost fully ionized; it has a density $N_e$ from $10^{12}$ to $10^{13}$ cm$^{-3}$ and a temperature $T_e$ from 4 to 10 eV. The plasma can be maintained for any value of the magnetic field strength exceeding that corresponding to electron cyclotron resonance in the region of the plasma source. The latter is placed halfway between the maximum and the minimum values of the mirror field. The whistler wave is launched either by the same slow-wave structure used to produce the plasma or by a second similar structure placed at the other end of the mirror magnetic field.

This unique property of the experiment affords the following advantages: (i) In the presence of the plasma the structure is an excellently matched, extremely broad-band device allowing experimental observation of whistler modes over a wide range of plasma parameters. (ii) Direct coupling of the test wave between the wave-launching system and a receiving antenna is completely avoided by choosing free-space wavelengths much larger than the internal diameter of the slow-wave structure. (iii) Efficient coupling of the test wave to the plasma permits easy detection of the plasma wave by means of conventional instrumentation.

The test wave is detected by an axially movable coaxial probe immersed radially in the plasma. The wave propagation path between the wave-launching system and the probe forms one branch of a variation[7] of a Wharton interferometer.

In Figs. 1(a) and 1(b) the lower trace displays the amplitude of the test wave along a propagation path of 10 cm, the zero point to the left of both figures corresponding to the center of the mirror. The upper traces of Figs. 1(a) and 1(b) show the multiple fringes of the interferometer due to the phase shift along the same path. The fringe calibration is $2\pi$/cm. The wave was launched from the right at a distance of 15 cm from the center of the mirror.

The values of $\omega_b/\omega$ derived from the geometry of the magnetostatic field and from the frequency of the test wave are given on the abscissas of both figures to correspond with the propagation

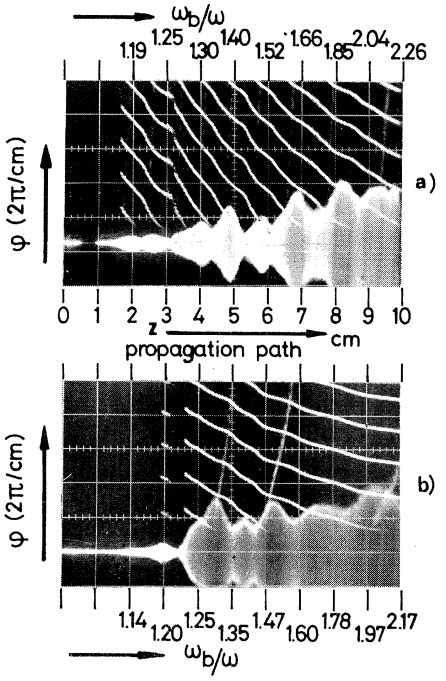


FIG. 1. (a) Collisional discharge, (b) noncollisional discharge. Upper traces: Phase shift of the test wave along its propagation path (from the right to left). Lower traces: Amplitude variation of the test wave.

path $z$ marked in centimeters. The $z$ incremental phase shift $d\varphi$ of the test wave should be described by the relation

$$d\varphi = k_z dz = (2\pi/\lambda)n(z)dz, \qquad (2)$$

where $\lambda$ is the free-space wavelength and the refractive index $n(z)$ is given by Eq. (1) by inserting the $\omega_b/\omega$ values corresponding to $z$. Thus the slope of the phase-shift displays of Figs. 1(a) and 1(b) gives $n(z)$ *directly* at each point of the propagation path. With the corresponding values of $\omega_b/\omega$ marked in Figs. 1(a) and 1(b), $n(\omega_b/\omega)$ can be plotted immediately in terms of Eq. (1). The hitherto cumbersome measurement of $n(\omega_b/\omega)$ in a uniform magnetic field is thereby avoided.[2]

Figure 2 shows $n$ vs $\omega_b/\omega$ for three different values of $\omega_p/\omega$, two of them, labeled (a) and (b), being derived from Figs. 1(a) and 1(b), respectively. The amplitude of the test wave for $\omega_p/\omega = 5.5$, which is directly recorded versus $z$ in Fig. 1(b), is also given in Fig. 2, curve $b$, as a function of $\omega_b/\omega$. The values of $\omega_p/\omega$ resulting from the dispersion curves of Fig. 2 agree well with the density derived from measurements of ordinary transverse wave propagation.[7] Figure 2 clearly demonstrates that when the wavelength of the plasma waves becomes smaller than or

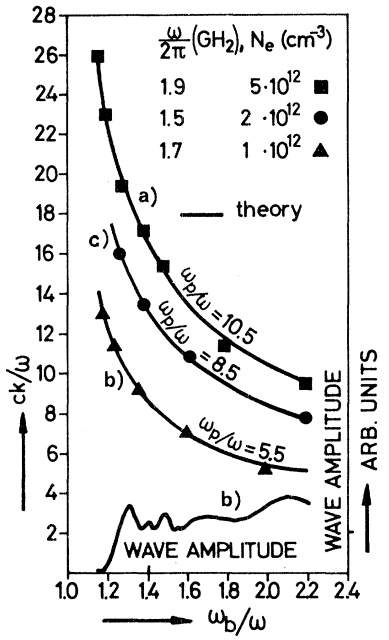


FIG. 2. Dispersion and damping of the test wave for three different values of $\omega_p/\omega$.

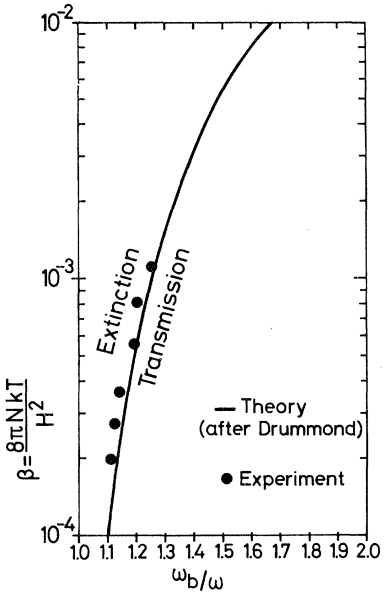


FIG. 3. Shift in the onset of transmission from $\omega_b/\omega = 1$.

comparable to the transverse dimensions of a laboratory plasma, the dispersion characteristics of these waves approach those of the corresponding plane waves in an unbounded plasma. Using free-space wavelengths $\lambda$ much larger than the vacuum cutoff dimension of the wave launching device, it is possible to choose $\omega$ for a fundamental mode of propagation along the plasma waveguide. Measurements taken radially to the plasma column show a bell-shaped amplitude variation of the test wave localized in the central core of the plasma, where the density and hence the refractive index of the plasma is highest.

Preliminary data on wave-absorption measurements are shown in the lower traces of Figs. 1(a) and 1(b) for collisional and noncollisional wave damping, respectively. In the collisional case the wave is progressively absorbed along its propagation path, while in the noncollisional case the absorption of the wave is more related to the low phase velocity of the whistler wave near the cyclotron resonance region. The amplitude discontinuities in both figures may be due to partial reflection of the wave at the plasma boundary or to the building up of higher modes of propagation in regions of higher refractivity.

As shown by Drummond,[3] one effect of nonzero electron temperature is that the refractive index is complex for frequencies less than the electron cyclotron frequency. For low values of electron temperature, the dispersion relation of Eq. (1), which is valid for collisionless plasmas, is also valid to a first approximation for the low temperature range of 4 to 10 eV in this discharge. But the sharp transition from attenuation to transmission, revealed by the lower trace of Fig. 1(b), suggests a check of Drummond's predictions, which give the shift in the onset of transmission from $\omega_b/\omega = 1$ as a function of $\beta = 8\pi nkT/H^2$. The result of this comparison, shown in Fig. 3, reveals a fair coincidence of the measured $\beta$ values with that predicted by Drummond. The data are derived for several $nkT$ values, either from measurements similar to that in Fig. 1(b) or from direct measurements of the onset of transmission between two fixed points of the discharge.

As predicted by the theory, no variation of the transmission onset is noted when, while keeping $\beta$ constant, the density and the temperature of the discharge are varied.

Instead of a receiving probe immersed in the plasma, preliminary measurements made with two $L$ coils[6] as transmitting and receiving antennas already suggest the possibility of using whistler modes or helicon waves for $\beta$ measurements in fusion devices, as proposed by Drummond.[3]

---

[1]T. H. Stix, *The Theory of Plasma Waves* (McGraw-Hill, New York, 1962).

[2]F. W. Crawford, Stanford University Institute for Plasma Research Report No. 256, 1968 (unpublished).
[3]J. E. Drummond, Phys. Rev. 112, 1460 (1958).
[4]M. P. Bachynski and B. W. Gibbs, Phys. Fluids 9, 520, 532 (1966).
[5]D. C. Mahaffey, Phys. Rev. 129, 1481 (1963).
[6]G. Lisitano, M. Fontanesi, and E. Sindoni, Appl. Phys. Lett. 16, 122 (1970).
[7]A. Capitanio, E. Rossetti, and G. Lisitano, to be published.

# Specific Heat and Resistivity Near the Order-Disorder Transition in β-Brass*

D. S. Simons and M. B. Salamon†
*Department of Physics and Materials Research Laboratory, University of Illinois, Urbana, Illinois 61801*
(Received 8 February 1971)

The specific heat and temperature derivative of the resistivity of β brass have been simultaneously measured near its order-disorder transition and found to be proportional. An extension of the Fisher-Langer theory for magnetic transitions is used to explain the results.

Several years ago Fisher and Langer predicted that the contributions to the specific heat and temperature derivative of the electrical resistivity associated with a magnetic phase transition are proportional.[1] This prediction has been verified for the ferromagnetic transition in nickel,[2,3] but seems to fail for the antiferromagnetic transitions in chromium[4] and dysprosium,[5] at least in their polycrystalline forms.

We have chosen to investigate in detail the specific heat and resistivity near the order-disorder transition in β brass for the following reasons: (1) The temperature derivative of the resistivity is known to have the same qualitative behavior as the specific heat.[6,7] (2) The specific heat of β brass has been accurately measured[8] and can be used as a check of our results. (3) High-quality samples were available to us. (4) The Fisher-Langer theory can be applied to order-disorder transitions in binary alloys.

The ac calorimetry technique used by Ashman and Handler to measure the specific heat of β brass[8] has been extended to include a simultaneous determination of the temperature derivative of the resistivity. In this method, a small sample is periodically heated with chopped light from a quartz-iodide bulb. In the proper frequency range (19 Hz was used in this experiment), the amplitude of the temperature oscillations of the sample is inversely proportional to its specific heat. These oscillations are detected by a Chromel-Constantan thermocouple with one junction spot welded to the sample and the other attached to a heat sink at the ambient furnace temperature. The amplitude of oscillations is measured with a lock-in amplifier whose output is recorded on a multipoint chart recorder. A second Chromel-Constantan thermocouple with one junction spot welded to the sample and the other in an ice bath monitors the dc temperature of the sample. This thermocouple voltage is measured with a potentiometer using a microvoltmeter as a null detector, and recorded as a second trace on the chart recorder.

The temperature derivative of the resistivity is obtained at the same time as the specific heat by passing a constant current of 0.26 A through the sample. The voltage oscillations induced by the temperature oscillations of the sample are detected with a second lock-in amplifier and recorded as the third trace on the chart recorder. After measuring the dc voltage drop across the sample at 25°C, one has the geometry-independent quantity

$$\alpha_R(T) \equiv \frac{1}{\rho_{25°C}} \left(\frac{d\rho}{dT}\right)_p \simeq \frac{1}{V_{25°C}} \frac{\Delta V(T)}{\Delta T(T)}, \qquad (1)$$

where $\Delta V$ and $\Delta T$ are the magnitudes of the voltage and temperature oscillations, respectively, at temperature $T$. Good temperature resolution is achieved since the rms temperature oscillations are typically 0.01°K near the transition temperature.

The sample of β brass used in this experiment was cut from the same boule used by Ashman for his specific-heat measurements.[8] It contained 52.3 ± 0.1% Cu and 47.7 ± 0.1% Zn. A sample was spark cut and thinned by mechanical and electropolishing techniques to final dimensions 6.0 mm × 1.5 mm × 0.1 mm. It was blackened with a thin layer of Aquadag graphite dispersion for maximum absorption of the light and mounted in a modified version of Ashman's sample holder.[8,9]

Results of the measurements are shown in

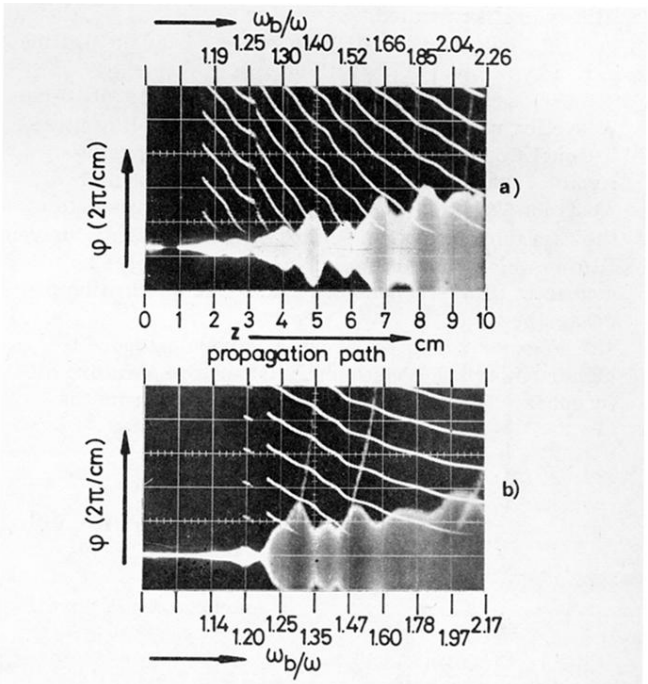


FIG. 1. (a) Collisional discharge, (b) noncollisional discharge. Upper traces: Phase shift of the test wave along its propagation path (from the right to left). Lower traces: Amplitude variation of the test wave.